

Prediction of Behavior of Organic Rankine Cycle Driven Concentrated Power Collectors with Magnetized Nanofluid CuO

S. Sami^{1,2,3}

Professor, and Founder

¹TransPacific Energy, Inc, NV, US 89183

²IES, University of North Dakota, Grand Forks, ND, 58202

Abstract: *The behavioral performance of magnetized nanofluids CuO in Parabolic Trough Concentrating Solar Collector (CSP) with an Organic Rankine Cycle (ORC), and a Thermal Energy Storage (TES) system were studied under different solar radiations. The ORC uses an environmentally sound quaternary mixture composed of R134a, R245fa, R125, R236fa. The results showed that the power output and Hybrid efficiency of the CSP collector and thermal energy stored in the storage tank were enhanced with the increase of the solar radiation and the magnetic field force. Also, the study concluded that the magnetized nanofluid CuO outperformed other nanofluids under study under similar conditions. Finally, the model's prediction compared fairly with data reported in the literature.*

Keywords: CSP solar collectors, magnetized nanofluids, magnetic field, Organic Rankine Cycle, modeling, simulation, and model's validation

1. Introduction

As energy demand across the globe increases, harnessing renewable energy remains essential. Concentrating sunlight is an effective way to generate higher output and nanofluids can play a crucial role in the development of these technologies. Concentrating solar power collectors (CSP) has received significant attention for electricity generation and heat production capability. "Thermal storage integrated CSP overcomes the intermittency of solar radiation. The thermophysical properties of the heat transfer fluids (HTF) and the thermal energy storage (TES) materials are key to enhancing the CSP system's efficiency [1-49]. In general, the CSP power generation systems use solar concentrators to focus solar radiation onto a receiver that carries a heat transfer fluid which is heated up to a high temperature due to high concentrated solar radiation. Generally, in most CSP plants, the heat transfer fluid is thermal oil. This heat transfer fluid goes to a conventional steam turbine using water as coolant or an Organic Rankine Turbine generator, ORC, using refrigerant, where electricity is generated [1, 7]. Thermal energy storage is an integral part of a CSP plant, to overcome the intermittency of solar radiations for continuous production of power during the night, and on cloudy days" [8,9]. Moreover, Sami [10], studied the performance of "nanofluids Al₂O₃, CuO, Fe₃O₄, and SiO₂ in a Parabolic Trough Concentrating Solar Collector (CSP)-based power generation plant, an Organic Rankine Cycle (ORC), and a Thermal Energy Storage (TES) system. The results showed that the power collected by the CSP collector, hybrid thermal efficiency, and thermal energy stored was enhanced with the increase of solar radiation. Also, the study concludes that the nanofluid CuO outperformed the other nanofluids. Thermodynamic modeling of ORC has been reported in the literature by different authors including Saloux et al. [23] and Sami [24, 25]. In this paper, a numerical model was presented to "simulate and study the behavior of different magnetized

nanofluids circulating in the parabolic trough solar collector loop to drive an Organic Rankine Cycle using an environmentally quaternary refrigerant mixture, under different solar radiations. The model has been established after the mass and energy equations written for magnetized nanofluids; Al₂O₃, CuO, Fe₃O₄, and SiO₂. These conservation equations were coupled with equations ORC and thermal storage under different operating conditions. This research represents a significant contribution to nanofluid science with the magnetic field.

2. Mathematical Model

The schematic in Figure.1 depicted the proposed CPS system which is composed of a CPS solar collector, thermal storage tank, piping, and pump as well as the waste heat boiler of the ORC. The solar radiation is absorbed by the CSP solar collector and converted into thermal energy that heats the magnetized nanofluids and thermal oil circulating to the thermal oil/storage tank loop. The thermal oil drives the Organic Rankine Cycle ORC and evaporates the refrigerant blend in the waste heat boiler that is used to drive the ORC vapor turbine to generate power. The condensed blend vapor in the condenser is pumped back to the waste heat boiler to complete the ORC cycle". "The refrigerant mixture used in the ORC loop is an environmentally sound quaternary mixture composed of R1234yf, R245fa, R125, R236fa developed and reported by Sami [28]. Thermodynamic and thermophysical properties were obtained at REFPROP [33]. One of the most important characteristics of the mixture R1234yf, R245fa, R125, R236fa, are the variable saturation temperature and glide temperature that are pivotal in absorbing more thermal energy at low-grade temperatures and enhancing the Organic Rankine Cycle efficiency". For the magnetized nanofluids heat transport fluid. It is assumed in the model that; the magnetized nanofluid is homogeneous, isotropic, incompressible, Newtonian, and inlet velocity and inlet

temperature are constant, and thermophysical properties of the magnetized nanofluids are constant.

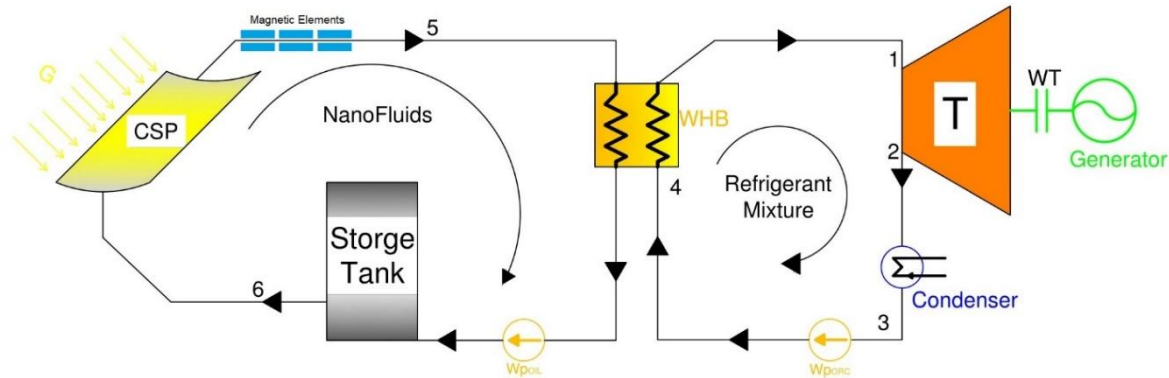


Figure 1: Flow diagram of the proposed CSP with magnetized nanofluids system

CSP Solar Collector Model:

The power absorbed from solar radiation by the CSP solar collector can be determined by the following [3-6, 23- 32];

$$P_{abs} = DNI * \cos \theta * \eta_{opt} * IAM * R_s * E_L * SF_{Avail} \quad (1)$$

Where;

DNI: Solar radiation (w/m2), θ : Angle of incidence, η_{opt} : Optical efficiency, IAM: Incidence angle modifier., R_s : Row shadow, E_L : End losses, and SF_{Avail} : Solar field available. The CSP collected power is given by [30];

$$P_{collector} = P_{abs} - P_{loss_{col}} - P_{loss_{pip}} \quad (2)$$

Where;

P_{abs} : Collector power absorbed by CSP defined in equation (1), $P_{loss_{col}}$: Collector thermal losses of the CSP., $P_{loss_{pip}}$: solar field piping losses. The CSP collector thermal losses outlined in equation (2) were calculated as reported in reference [30]. Readers interested in the details of the losses experienced by the CSP collector are advised to consult references [3-6, 23, 30-32]. The mass flow rate of the basic heat transfer fluid, thermal oil, can be given by the following;

$$m_{oil} = \frac{P_{collected} A_{aperture}}{C_{p_{oil}} (T_{field_{outlet}} - T_{field_{inlet}})} \quad (3)$$

Where, $A_{aperture}$: is the total aperture (m^2) and $T_{field_{outlet}}$ and $T_{field_{inlet}}$ are the outlet and inlet temperature of the thermal oil in the solar field. DOWTHERM thermal oil fluid was used in this simulation model [30-37];

$$Q_{storage\ tank} = \eta m_{oil} (T_5 - T_6) C_{p_{oil}} \quad (4)$$

Where m_{oil} is the oil flow rate obtained from equation (8) and $C_{p_{oil}}$ is the specific heat of thermal oil the base fluid. The thermal heat that can be discharged during the discharging process is [30-37];

$$Q_{storage\ tank} = m_{oil} (T_{hot\ tank} - T_{cold\ tank}) C_{p_{oil}} = \eta m_{salt} T_{hot\ tank} - T_{cold\ tank} C_{p_{salt}} \quad (5)$$

Where; m_{salt} ; the mass of salt in the storage thermal tank, and η : Efficiency of heat exchanger

The following energy balances at the ORC cycle as shown in Figure, 1 can be given in the following [23,32];

$$W_{ORC} = m_{ref} (h_1 - h_2) \quad (6)$$

$$Q_{WHB} = m_{ref} (h_1 - h_4) \quad (7)$$

$$Q_{COND} = m_{ref} (h_2 - h_3) \quad (8)$$

$$W_{PORC} = m_{ref} (h_4 - h_3) \quad (9)$$

Where, h_1 : enthalpy at the outlet of the waste heat boiler (KJ/Kg), h_2 : enthalpy at the exit of the vapor turbine (KJ/Kg), h_3 : enthalpy at the condenser outlet (KJ/kg), h_4 : enthalpy at ORC pump outlet (KJ/kg), and m_{ref} : refrigerant mass flow rate (kg/s). The ORC cycle thermodynamic properties were calculated using the REFPROP program [23,27, 30] using variable saturated boiling and condensation temperatures. The ORC efficiency can be calculated as;

$$\eta_{ORC} = \frac{W_{ORC} - W_{PORC}}{Q_{WHB}} \quad (10)$$

Where, W_{ORC} and W_{PORC} represent the work produced by the ORC and the work used by the ORC pump., and Q_{WHB} : Thermal energy supplied by the waste heat boiler.

$$\eta_{CSP} = \frac{Q_{abs}}{Q_{CSP}} \quad (11)$$

Where, W_{poil} : work used by the thermal oil pump, and Q_{CSP} is the CSP power collected and defined by equation (1). Finally, the hybrid efficiency of the CSP-ORC system is;

$$\eta_{SH} = \frac{W_{ORC} - W_{PORC} - W_{P_{oil}}}{Q_{collector}} \quad (12)$$

Where $Q_{collector}$ represents the collected CSP power and is given by equation (2).

Nanofluid heat transfer Fluid

Magnetized Nanofluids have been added to the “thermal oil heat transport base fluid to enhance its thermal properties. Sharma et al. [28], Sami [26,30-36], and Marefati et al. [37] presented the equations to calculate the thermophysical and thermodynamic properties of magnetized nanofluids”;

$$\alpha_{total} = \alpha_{particles} + \alpha_{base\ fluid} \quad (13)$$

Where α represents a thermophysical property of the nanofluid under investigation. The nanofluid thermal and thermophysical properties, α_{total} , can be calculated as follows;

$$\alpha_{total} = \alpha_{base\ fluid} + \alpha_{particles} (\Phi) \quad (14)$$

Where; Φ represents the nanoparticle's volumetric concentration.

The thermal conductivity is related to thermal diffusivity and density of the nanofluids as follows;

$$\lambda = \alpha \delta C_p \quad (15)$$

Where C_p is the specific heat, α is the thermal diffusivity, λ and ρ represent the thermal conductivity and density, respectively. Equations (13) through (15) can be used to

determine other thermophysical properties such as; α is the thermal diffusivity, k and ρ represent the thermal conductivity and density as different magnetic forces Gauss

published in the literature properties ([9], [10], [20]) as a function of the properties outlined in the Table.1

Table 1: Thermophysical Properties of magnetized nanofluids

	Ai2O3	CuO	Fe3O4	SiO2
C_{pnf}	$b = 0.1042a + 6226.5$	$b = 0.2011a + 5730.8$	$b = 0.8318a + 4269.8$	$b = 0.6187a + 4293.2$
K_{nf}	$b = 2E-05a + 1.4888$	$b = 5E-05a + 1.3703$	$b = 0.0002a + 1.0209$	$b = 0.0001a + 1.0265$
h	$b = 0.0031a + 73.092$	$b = 0.0031a + 73.073$	$b = 0.003a + 73.225$	$b = 0.003a + 73.231$

Where “b” represents the nanofluid specific property and “a” is the magnetic field force in Gauss. C_{pnf} , K_{nf} , and h are the specific heat, thermal conductivity, and heat transfer coefficients of nanofluids.

Numerical Procedure

The logical diagram presented in Figure.2 described the sequence of steps and calculations of the model. The equations (1) through (15) were integrated into the finite-difference formulations. Iterations were performed using MATLAB iteration techniques until a converged solution is reached with an acceptable iteration error of 0.05. The logical diagram starts with inputting solar radiations, nanofluids, magnetic field, system specifications, and parameters to initiate the calculation of the heat transport fluid characteristics in the CSP collector, thermal oil flow, storage tank, refrigerant flow, and finally, the ORC work and hybrid system efficiencies were calculated”.

3. Discussion and Analysis

“Hybridizing concentrating solar power and magnetized nanofluids technologies can lead to higher aggregate efficiencies over the typical efficiencies of 15%. Thereafter, in the following we use different solar radiations; 283, 599, and 189 w/m², at different angles of incidence at 8 AM, 12 PM, and 4.00 PM and magnetized nanofluid CuO and magnetic fields of 127 through 3000 Gauss, using thermal oil as heat transport fluid. It was assumed that the CSP Aperture is 510120 (m²) and the supply and exit temperatures to the CSP collector are 166.5 °C (331 °F) and 149.5 °C (301 °F), respectively, and ambient temperature of 25 °C (77 °F). Other output temperatures of the CSP solar collector were considered; 182 °C (361 °F), and 199 °C (391 °F)”. The “characteristics of the CSP hybrid system using thermal oil as heat transport base fluid were presented in Figures 3 and 4. at three different hours during the day, and different angles of incidence of the solar radiation in January 2018; 17.44° at 8:00 AM, 77.44° at 12:00 PM and 137.44° at 16:00. These figures showed that the maximum power absorbed by the CSP and ORC work output occurred during the mid-day.” Furthermore, it also showed that the higher the solar radiation the higher the characteristics of the CSP system and the power produced by the ORC. Results also demonstrated that the maximum efficiencies of the CSP and the hybrid system occurred at mid-day. This is because higher solar radiation at a higher angle of incidence increases the thermal energy absorbed by the CPS collector and the thermal energy delivered to the waste heat boiler of the ORC. This, in turn, increased the ORC work produced and the efficiencies of the CPS and the hybrid system efficiency of CSP”. The results also demonstrated that the maximum efficiencies occurred at noon and solar radiation of 599.67 w/m². Magnetized and non-magnetized “nanofluids such as CuO, Fe3O4, and SiO2 have received significant attention in the literature namely [10-32]. It has

been reported that CuO nanofluid has shown great enhancement when used as heat transport fluid. This obviously can be attributed to the higher thermodynamic, thermophysical and heat transfer properties of the nanofluid CuO [10-32].” Figures .3 through .8 showed that the nanofluid CuO enhanced the characteristics performance of the CSP solar collector system over the thermal oil as base heat transfer fluid. It appears from these figures that the higher the concentration of the magnetized nanofluid CuO the higher the ORC work produced. This resulted in enhancing the hybrid CSP solar collector system efficiency and other characteristics of the CSP under study. It can also be concluded, the higher the magnetized nanofluid CuO concentrations the higher the hybrid system performance characteristics. Furthermore, Figures 9 through .11 demonstrated that the higher the concentration of the magnetized nanofluid CuO the higher the CSP system characteristics such as ORC’s work, thermal energy at storage tank, and thermal energy supplied to the waste heat boiler of the ORC and also at the mid-day where solar radiation is the highest at 599.67 w/m². Also indicated that the higher efficiencies of the hybrid system the higher the solar radiations, but, the CSP collector efficiencies are independent of the nanofluid concentrations as per equation (11). Furthermore, The characteristics of the CSP collector system under solar radiations of 500, 750, 1000, and 1200 w/m² occurred at different hours of the day and different angles of incidence of the solar radiation; 17.44° at 8:00 AM, 77.44° at 12:00 PM, and 137.44° at 16:00. It is noted in Figures 12 through 14 that the ORC key parameters were enhanced with the increase of the solar radiation and at higher nanofluid concentrations as per Figures 3 through 11. However, it is to note that higher pressure head losses and pumping power losses in the thermal oil loop can increase at higher concentrations and that is undesirable. Therefore, the designer has to exercise caution when using the higher concentration of CuO nanofluid [25, 26, 30]”. The enhancement of the CSP solar collector system increased the ORC refrigerant mass flow rate and the hybrid system efficiency. It appears from Figures 12 through 14 that the higher the concentrations of nanofluids the higher the solar radiation, the higher the refrigerant mass flow rate, ORC work produced, and consequently the CSP hybrid system efficiency. Figures .12 through .14 illustrated the impact of the concentrations of nanofluid CuO on the performance of the ORC system and the CSP hybrid system under different solar radiations at the mid-day; 500, 750, 1000, and 1200 W/m². As seen in Figure.12, the thermal energy supplied by the CSP collector to the ORC loop has been enhanced with higher concentrations of this nanofluid at constant solar radiation, and consequently, the ORC work produced has

been also increased at higher concentrations. It is also found that the thermodynamic efficiencies with CuO nanofluid, under optimum conditions, are higher than those obtained from the base fluid. Also, the results displayed in this figure showed that the higher the solar radiation the higher the ORC output as illustrated in the figure.13 On the other hand, Figure.14 showed that the efficiency of the CSP solar collector hybrid system has been increased with the increase of solar radiation and as discussed earlier and is independent of the nanofluid concentrations as per equation (15). Finally, our results conclude that the combination of the ORC with the CuO nanofluid is the optimum choice for the CSP solar hybrid system which agreed with what has been reported in the literature namely; [31, 35].

Model validation:

Among a few experimental data that have been reported in the literature on the use of nanofluids in CSP solar collectors, we compared the present model's prediction of the enhancement ratio of the ORC work produced due to the use of the nanofluids; CuO with the data reported by Bellos

and Tzivanidis [41]. This comparison is presented in Figures.15 under nanofluid concentrations of 1% through 6%. The "experimental data of the trigeneration system studied by reference [41] included an organic Rankine cycle (ORC) and an absorption heat pump operating with LiBr-H₂O which is powered by the heat dissipated from the condenser of the ORC. The comparison was shown in Figure. ,15 between the data of Bellos and Tzivanidis [41] and our model's prediction was performed using the nanofluids CuO. It was found that the experimental data and the model have the same trend; however, some discrepancies existed between the model's prediction and the experimental data. It is believed that the selection of the basic operating parameters; such as the pressure in the turbine inlet, the temperature in the ORC condenser, and the nanofluid CuCO concentration is attributed to the discrepancies between the model's prediction and the data. In addition, Reference [41] did not fully disclose the aforementioned parameters which are critical to the validation of the current model. It is worthwhile that other references were consulted [36-40] to get details on these parameters".

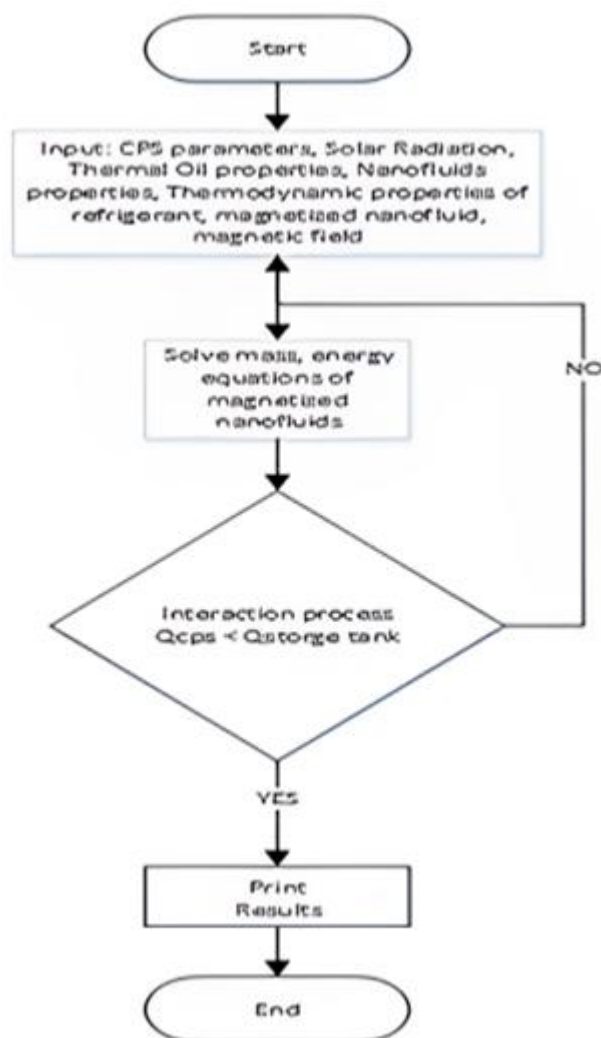


Figure 2: Logical block diagram for numerical model solution

4. Conclusions

This study investigated the enhancement effect and characteristics of nanofluid CuO, circulating concentrating solar power (CSP) with ORC, and Thermal Energy Storage

under different solar radiations, angle of incidence, and different CuCo concentrations. The results showed that the power absorbed, and collected by the CSP collector, thermal energy stored in the storage tank, and work produced by the ORC were enhanced with the increase of the solar

radiations. In addition, the CSP efficiency was peaked at the mid-day. It was also found that the CSP hybrid system efficiency has been enhanced mainly by the increase of solar radiation and at higher nanofluid concentrations and higher magnetic field force, over the thermal oil as base fluid. As expected, the results indicated that the CSP collector efficiencies were independent of the nanofluid concentrations. In addition, the study concluded that the magnetized nanofluid CuO outperforms other nanofluids reported in the literature and thermal oil base fluid under similar conditions. Finally, it was found that the model's prediction compared fairly with data reported in the literature; however, some discrepancies existed between the model's prediction and the experimental data. It is recommended that further experimental studies be conducted using magnetized the nanofluids Al_2O_3 , Fe_3O_4 , and SiO_2 in CSP solar collector loop to obtain more experimental data for the numerical validation under different solar radiations, magnetic fields, and heat transfer fluid under different conditions.

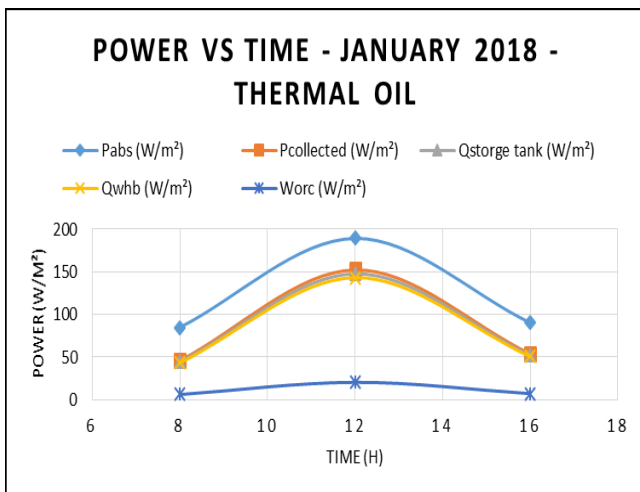


Figure 3: CSP hybrid system has different characteristics with thermal oil as a base fluid

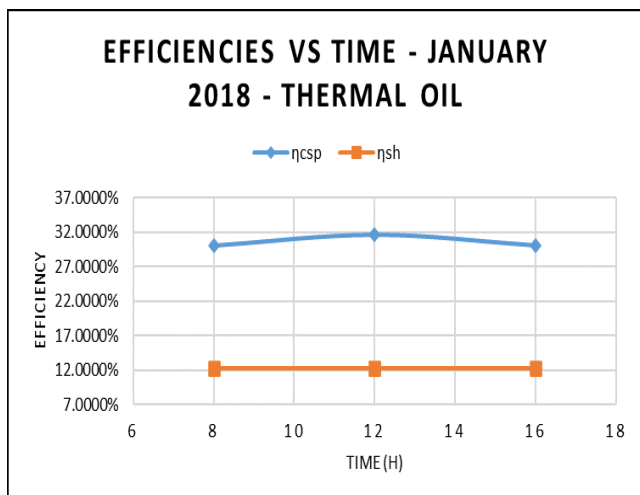


Figure 4: CSP hybrid system efficacies with thermal oil as base fluid

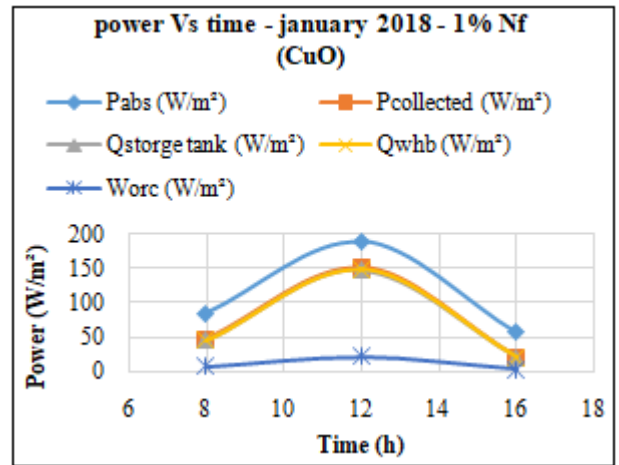


Figure 5: CSP hybrid system Characteristics with CuO 1% concentration and thermal oil as base fluid

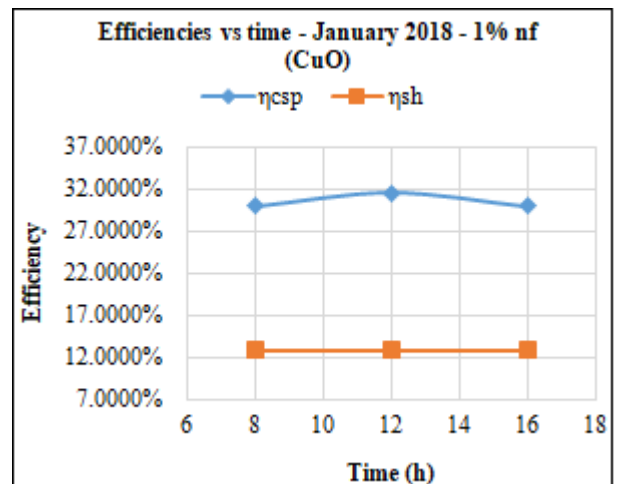


Figure 6: CSP hybrid system efficacies at CuO 1% with thermal oil as base fluid

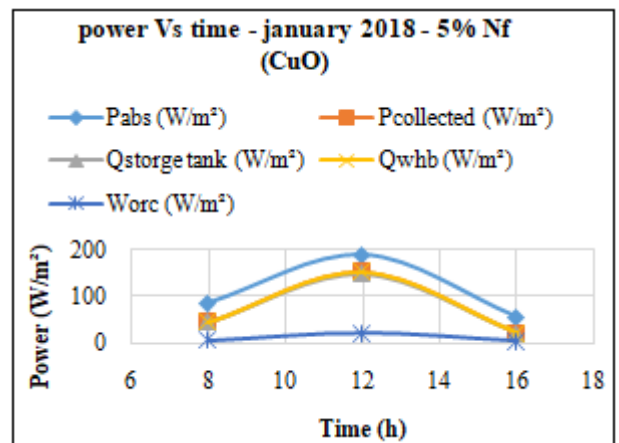


Figure 7: CSP hybrid system Characteristics at 5% CuO with thermal oil as base fluid

Nomenclature

- A_{aperture} : is the total aperture (m²)
- C_{poil} is the specific heat of thermal oil in the base fluid.
- DNI: Solar radiation (w/m²)
- E_j : End losses
- h_1 enthalpy at the outlet of the waste heat boiler (kj/Kg)
- h_2 : enthalpy at the exit of the vapor turbine (kj/Kg)
- h_3 : enthalpy at the condenser outlet (kj/kg)
- h_4 : enthalpy at ORC pump outlet (kj/kg)

m_{ref} : refrigerant mass flow rate (kg/s)

m_{oil} is the oil flow rate obtained from equation (8)

IAM: Incidence angle modifier.

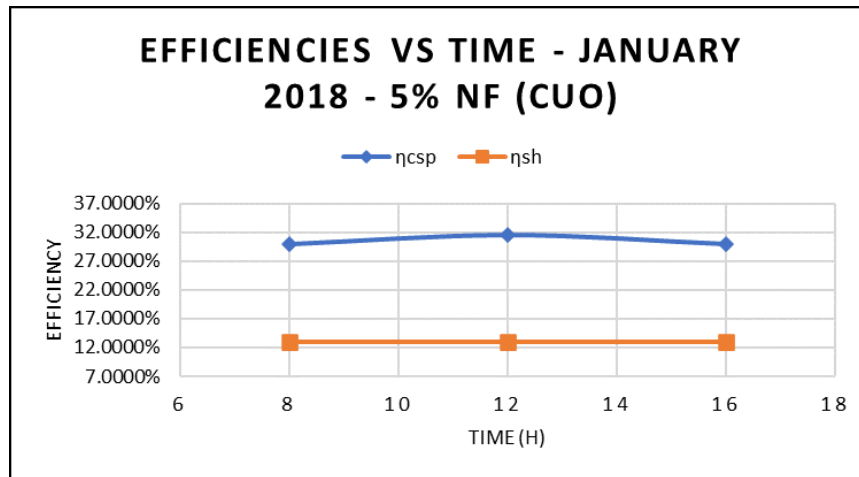


Figure 8: CSP hybrid system efficacies at 5% CuO with thermal oil as base fluid

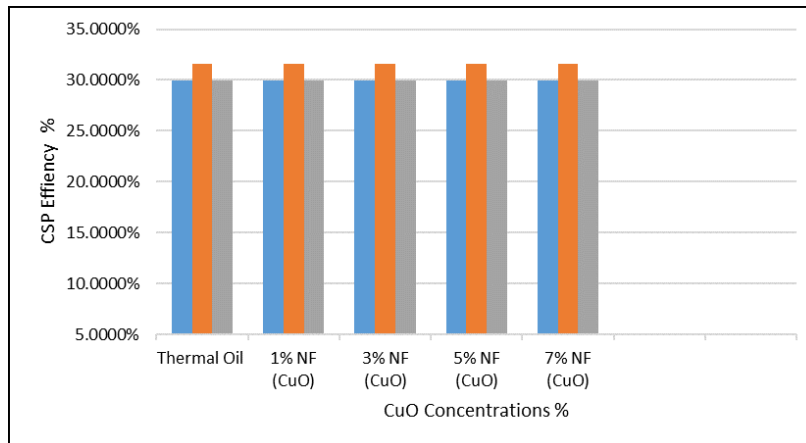


Figure 9: CSP efficacies at different CuO concentrations with thermal oil as base fluid

P_{abs} : Collector power absorbed by CSP defined in equation (1)

$P_{losscol}$: Collector thermal losses of the CSP.

$P_{losspip}$: solar field piping losses.

R_s : Row shadow

SF_{Aval} : Solar field available

Greek

Θ : Angle of incidence

η_{opt} : Optical efficiency

ρ_p represents the density of the nanoparticle.

Acknowledgment

The research work presented in this paper was made possible through the help of Edwin Martin, in conducting the numerical calculations.

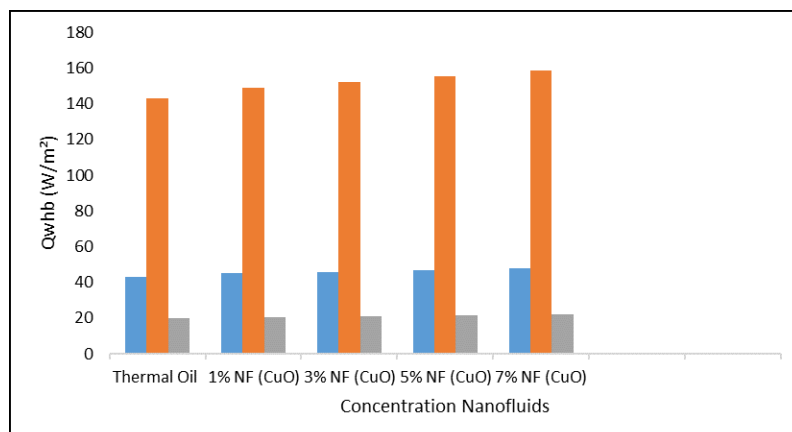


Figure 10: CSP hybrid system ORC waste heat boiler at different CuO concentrations

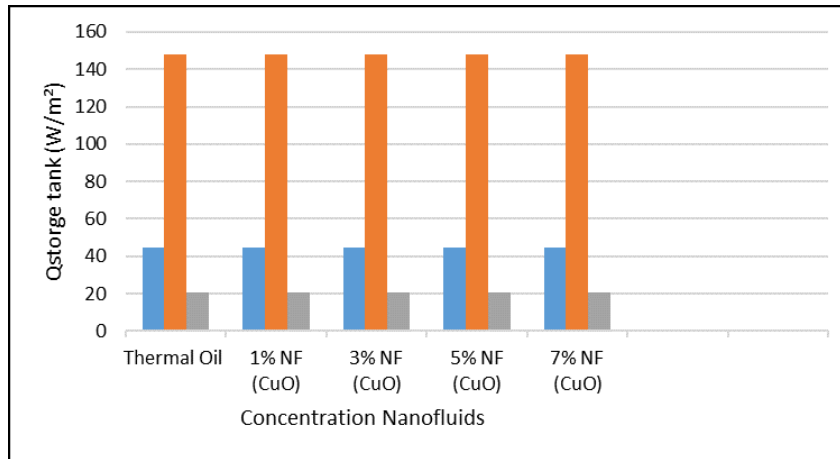


Figure 11: CSP hybrid system thermal energy Storage at different concentrations of CuO

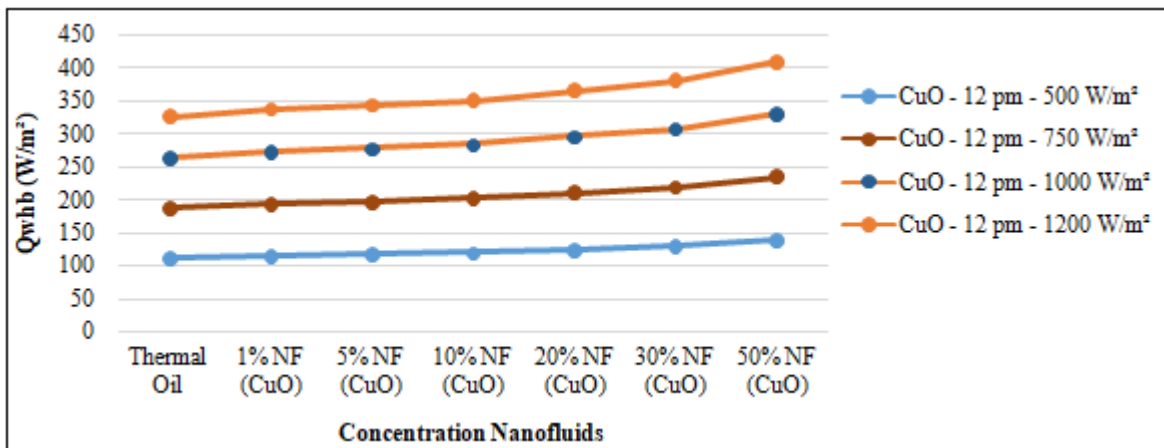


Figure 12: CSP system hybrid waste heat boiler thermal energy at CuO nanofluid -concentrations

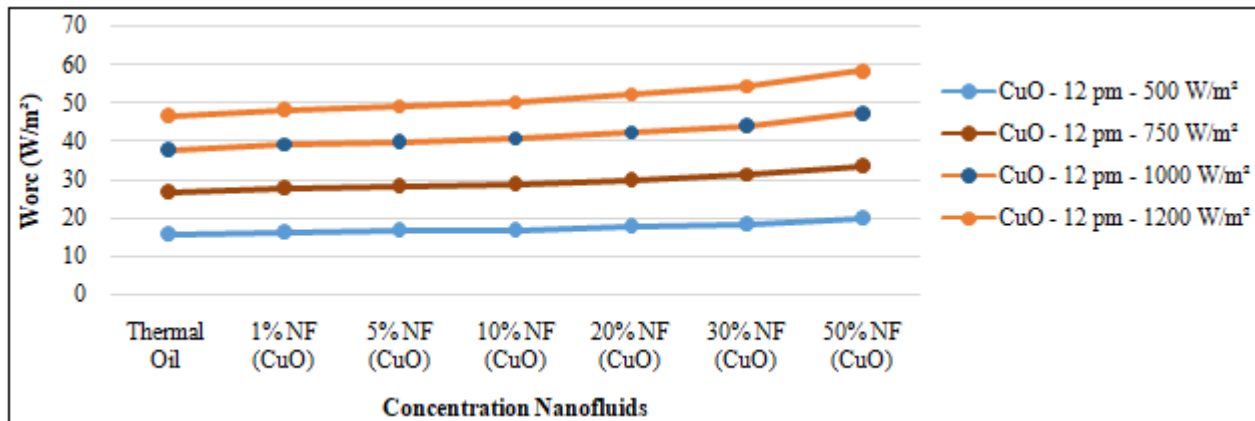


Figure 13: CSP system hybrid ORC work at CuO nanofluid and different concentrations

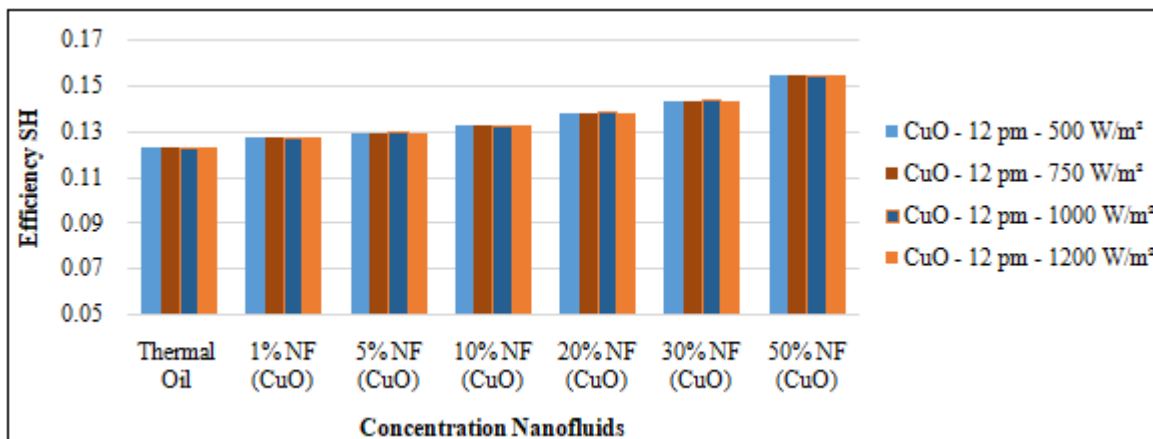


Figure 14: CSP system hybrid efficiency at CuO nanofluid and different concentrations

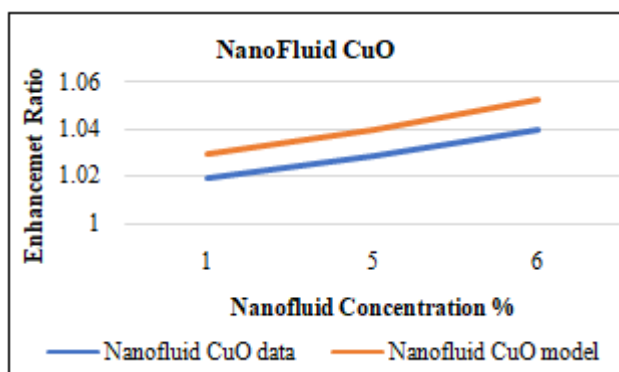


Figure 15: Comparison between model and data of Bellosand Tzivanidis[41].

References

- [1] Pavlović, TM, Radonjić IS, Milosavljević DD, Pantić LS. (2012), "A review of concentrating solar power plants in the world and their potential use in Serbia". *Renew Sustain Energy Rev* 2012; 16:3891–902.
- [2] S. Sami, (2021) Impact of Magnetic Field on the Dynamic Performance of Photovoltaic-Thermal Panel with Nanofluid, *Chemical Science International Journal*, 2021 – Volume 30 [Issue 6], Page 35-58, DOI: 10.9734/CSJI/2021/v30i63023, Published: 15 July 2021
- [3] S. Sami, (2020) Book; Applications of Nanomaterials in Human Health, Chapter 4: Application of Nanomaterials: Overview and Historical Perspectives Samuel Sami-Howard Pages 45-63 DOI <https://doi.org/10.1007/978-981-15-4802-4>.
- [4] Bahram Saadatfara, Reza Fakhraia, TorstenFranssona (2013), "Conceptual modeling of nanofluid ORC for solar thermal polygeneration" *Energy Procedia* 57 (2014) 2696 – 2705
- [5] Ummadisingu A, Soni M. (2011), "Concentrating solar power–technology, potential and policy in India". *Renew Sustain Energy Rev* 2011; 15:5169–75.
- [6] Izquierdo, S, Montanes C, Dopazo C, Fueyo N. (2010), "Analysis of CSP plants for the definition of energy policies: the influence on electricity cost of solar multiples, capacity factors, and energy storage", *Energy Policy* 2010; 38:6215–2.
- [7] Solar PACES. CSP projects around the world. Available from (<http://www.solarplaces.org/csp-technology/csp-projects-around-the-world>); 2016 [Last accessed on 07 May 2016].
- [8] Mohamad A, Orfi J, Alansary H. (2014), "Heat losses from parabolic trough solar collectors". *Int J Energy Res* 2014; 38:20–8.
- [9] Md TasbirulIslama, Nazmul Huda, A.B. Abdullah, R. Saidur, d, (2018), "A comprehensive review of state-of-the-art concentrating solar power (CSP), technologies: Current status and research trends", *Renewable and Sustainable Energy Reviews* 91 (2018) 987–1018
- [10] S. Sami, (2019) Analysis of Nanofluids Behavior in Concentrated Solar Power Collectors with Organic Rankine Cycle, *Appl. Syst. Innov.* 2019, 2, 0022; doi:10.3390/asi2030022 www.mdpi.com/journal/asi
- [11] Guannan Wang, Zhen Zhang, Ruijin Wang, and Zefei Zhu (2020), A Review on Heat Transfer of Nanofluids by Applied Electric Field or Magnetic Field, *Nanomaterials (Basel)*. 2020 Dec; 10(12): 2386. Published online 2020 Nov 29. doi: 10.3390/nano10122386
- [12] Peters M, Schmidt TS, Wiederkehr D, Schneider M. Shedding light on solar technologies—a techno-economic assessment and its policy implications. *Energy Policy* 2011; 39:6422–39.
- [13] M. Orosz, R. Dickes, (2017), "Organic Rankine Cycle (ORC) Power Systems, Technologies and Applications", 2017, Pages 569-612, <https://doi.org/10.1016/B978-0-08-100510-1.00016-8>
- [14] J. Freeman, I, Guarracinoa S.A, Kalogiroub C, N.Markidesa, (2017), "A small-scale solar organic Rankine cycle combined heat and power system with integrated thermal energy storage", *Applied Thermal*

- Engineering, Volume 127, 25 December 2017, Pages 1543-1554
- [15] R. A. Taylor, P. E. Phelan, Todd Otanicar, C. A. Walker, M. Nguyen, (2011), "Applicability of Nanofluids in High Flux Solar Collectors", *Journal of Renewable and Sustainable Energy*, 3(2), 2011.
- [16] P.K. Nagarajan, J. Subramani, S. Suyambazhahan, Ravishankar Sathyamurthy, (2014), "Nanofluids for solar collector applications: A Review", *Energy Procedia* 61 (2014) 2416 – 2434
- [17] F. Calise, and L. Vanoli, (2012), "Parabolic Trough Photovoltaic/Thermal Collectors: Design and Simulation Model", *Energies* 2012, 5, 4186-4208; doi:10.3390/en5104186
- [18] N. Bozorgan and M. Shafahi, (2015), "Performance evaluation of nanofluids in solar energy: a review of the recent literature", *NanoSystems Letters* (2015) 3:5 DOI 10.1186/s40486-015-0014-2
- [19] D. Shin, Byeongnam Jo, Hyun-eun Kwak, and D. Banerjee, (2010), "Investigation of High-Temperature Nanofluids for Solar Thermal Power Conversion and Storage Applications", Paper No. IHTC14-23296, pp. 583-591; 9 pages, doi:10.1115/IHTC14-23296, 2010 14th International Heat Transfer Conference, 2010 14th International Heat Transfer Conference, Volume 7, Washington, DC, USA, August 8–13, 2010
- [20] M. Lomascolo, G. Colangelo, M. Milanese, A. de Risi,(2015)," Review of heat transfer in nanofluids: Conductive,convective and radiative experimental results" *Renewable and Sustainable Energy Reviews* 43 1182–1198,2015.
- [21] M. Milanese, G.Colangelo, A.Creti, M.Lomascolo, F.Iacobazzi, A. de Risi: (2016), "Optical absorption measurements of oxide nanoparticles for application as nanofluid indirect absorption solar power systems-Part II: ZnO, CeO₂, Fe₂O₃ nanoparticles behavior" *Solar Energy Materials & Solar Cells* 147 321–326 (2016)
- [22] F. Iacobazzi, M. Milanese, G. Colangelo, M. Lomascolo, A. de Risi(2016), " An explanation of the Al₂O₃ nanofluid thermal conductivity based on the phonon theory of liquid" *Energy* 116 786-794, (2016)
- [23] B. Saadatfar, R. Fakhrai, and T. Fransson, (2014), "Conceptual Modeling of Nano Fluid ORC for Solar Thermal Polygeneration", *Energy Procedia*, Volume 57, 2014, Pages 2696-2705, <https://doi.org/10.1016/j.egypro.2014.10.301>
- [24] C. Tzivanidis, B. Evangelos and A. Antonopoulos, (2016), "Energetic and financial investigation of a stand-alone solar-thermal Organic Rankine Cycle power plan", October 2016, *Energy Conversion and Management* 126:421-433, DOI: 10.1016/j.enconman.2016.08.033
- [26] A. Alashkar and M. Gadall, (2018) "Thermodynamic Analysis of a Parabolic Trough Solar Collector Power Generation Plant Coupled with an Organic Rankine Cycle", ASME 2018 Power Conference collocated with the ASME 2018 12th International Conference on Energy Sustainability and the ASME 2018 Nuclear Forum; Paper No. POWER2018-7548, pp. V001T06A030; 11 pages, doi:10.1115/POWER2018-7548
- [27] E. Saloux, M. Sorin, H. Nesreddine, and A. Teysseidou, (2019), "Thermodynamic Modeling and Optimal Operating Conditions of Organic Rankine Cycles (ORC) Independently of the Working Fluid", *International Journal of Green Technology*, 2019, 5, 9-22.
- [28] Sami, S., and Marin, E., (2016); "A Numerical Model for Predicting Dynamic Performance of Biomass-Integrated Organic Rankine Cycle, ORC, System for Electricity Generation", *AJEE, American Journal of Energy Engineering*, Volume 4, No 3, p 26-33, 2016.
- [29] 28. Sami. S. (2011), "Behavior of ORC low-temperature power generation with different refrigerants". *Int J Ambient Energy*, 2011; 32: 37-45.<https://doi.org/10.1080/01430750.2011.584451>
- [30] Jo ao P. Silva and R. Castro, (2012), "Modeling and Simulation of a Parabolic Trough Power Plant", *January 2012 Green* 2(2):97-104, DOI: 10.1515/green-2011-0019
- [31] K.V. Sharma, Akilu Suleiman, Hj. Suhaimi B. Hassan and Gurumurthy Hegde, (2017), "Considerations on the Thermophysical Properties of Nanofluids", *Engineering Applications of Nanotechnology, Topics in Mining, Metallurgy and Materials Engineering*, DOI 10.1007/978-3-319-29761-3_2
- [32] S. Sami, (2018); Impact of magnetic field on the enhancement of performance of thermal solar collectors using nanofluids, *International Journal of Ambient Energy*, DOI: 10.1080/01430750.2018.1437561
- [33] S. Sami. (2019), Analysis of Nanofluids Behavior in Concentrated Solar Power Collectors with Organic Rankine Cycle, *Appl. Syst. Innov.* 2019, 2, 0022; doi:10.3390/asi2030022 www.mdpi.com/journal/asi<https://www.nist.gov/srd/refprop>, 2013
- [34] B. Prasartkaew, (2017), "Efficiency improvement of a concentrated solar receiver for water heating system using porous medium", *IOP Conf. Series: Materials Science and Engineering* 297 (2017) 012059 doi:10.1088/1757-899X/297/1/012059
- [35] S. Sami and E. Marin, (2019), "Modelling and Simulation of PV Solar-Thermoelectric Generators using Nanofluids", *International Journal of Sustainable Energy and Environmental Research*, Vol. 8, No. 1, pp. 10-28, 2019, DOI: 10.18488/journal.13.2019.81.10.28.
- [36] X. Zhang, Yuting Wu, Chongfang Ma, Q. Meng, X. Hu, and C. Yang, 2019, "Experimental Study on Temperature Distribution and Heat Losses of a Molten Salt Heat Storage Tank", *Energies* 2019, 12(10), 1943; doi:10.3390/en12101943
- [37] M. Marefati, M. Mehrpooya, M. Behshad Shafii, (2018), "Optical and thermal analysis of a parabolic trough solar collector for production of thermal energy in different climates in Iran with a comparison between the conventional nanofluids", *Journal of cleaner production* 175, (2018), 294-313, (2018).
- [38] R. Wang, L. Jiang, Zhiwei Ma, A. Gonzalez-Diaz, Y. Wang and, Anthony Paul Roskilly, (2019), "Comparative Analysis of Small-Scale Organic Rankine Cycle Systems for Solar Energy

- Utilisation”, *Energies* 2019, 12, 829; doi:10.3390/en12050829 (2019).
- [39] R. Dickes, O. Dumont, S. Declaye, S. Quoilin, I. bell, Vincent, (2014), “Experimental investigation of an ORC system for a micro-solar power plant”, 22nd International Compressor Engineering Conference at Purdue, July 14-17, 2014, # 1604, pages 1-10.
- [40] B. Saadatfara, R. Fakhrai, T. Fransson, (2014), “Conceptual modeling of nanofluid ORC for solar thermal polygeneration”, *Energy Procedia* 57 (2014) 2696 – 2705, 2013 ISES Solar World Congress.
- [41] E. Bellos and C. Tzivanidis, (2017), “Optimization of a Solar-Driven Trigenation System with Nanofluid-Based Parabolic Trough Collectors”, *Energies* 2017, 10, 848; doi:10.3390/en10070848, (2017).
- [42] Incropera, Frank P.; DeWitt, David P. (2000). *Fundamentals of Heat and Mass Transfer (4th ed.)*. New York: Wiley. p. 493. ISBN 978-0-471-30460-9.
- [43] Heat Transfer Fluid - Dow Chemical, <https://www.dow.com/webapps/lit/litorder.asp?filepath=/heattrans/pdfs/noreg/>
- [44] 44Xu, Z.Y.; Wang, R.Z.; Wang, H.B. Experimental evaluation of a variable effect LiBr-water absorption chiller designed for the high-efficient solar cooling system. *Int. J. Refrig.* 2015, 59, 135–143.
- [45] Bellos, E.; Tzivanidis, C.; Antonopoulos, K.A. (2017) Exergetic, energetic and fine evaluation of a solar-driven absorption cooling system with various collector types. *Appl. Therm. Eng.* 2016, 102, 749–759.
- [46] F-Chart Software, Engineering Equation Solver (EES), 2015. Available online: <http://www.fchart.com/ee> (2017).